

Methanol- and Ethanol-Induced Convex Deformation and Macrovoid Formation of Poly(Methyl Methacrylate)

C. B. Lin,¹ C. S. Chen,² Zhi-Hong Chen,¹ Nan-Ching Su¹

¹Department of Mechanical and Electro-Mechanical Engineering, Tamkang University, Tamsui, Taipei, Republic of China

²Department of Aerospace Engineering, Tamkang University, Tamsui, Taipei, Republic of China

Received 2 December 2003; accepted 25 March 2004

DOI 10.1002/app.20772

Published online in Wiley InterScience (www.interscience.wiley.com).

ABSTRACT: Methanol- and ethanol-induced convex deformation and macrovoid formation in poly(methyl methacrylate) (PMMA) through sandwich structures, consisting of polycarbonate (PC)/PMMA/PC was investigated. The sandwich structures had a circular hole on the outer PC layer, which allowed the solvent to contact with PMMA. Both single-convex and double-convex deformations of the PMMA layer were produced, depending upon the hole diameter. For a fixed hole diameter, there was an optimum PMMA thickness, which produced maximum curvature for the double-convex deformation. The physical mechanism

for these phenomena can be well explained by the relative strength of the swelling stress and the deformation resistance of the PMMA layer. We also used the wet phase-inversion method to produce porous convex deformation for the sandwich structures. The size, number, and location of the convex pores can be prescribed. This may have potential applications in local filtering and other areas. © 2004 Wiley Periodicals, Inc. *J Appl Polym Sci* 93: 2254–2261, 2004

Key words: poly(methyl methacrylate); polycarbonate; diffusion; microdeformation

INTRODUCTION

The diffusion or mass transfer of an organic solvent into a polymer is influenced by diffusion-induced mechanical stress in the polymer and the chemical potential energy. The existence of the chemical potential energy gradient helps the solvent molecules to diffuse into the polymer. When the solvent diffuses into the polymer, it forces the molecular chains of the polymer to relax, migrate, and reorganize. The large-scale movement and rearrangement of molecular chains, or swelling, produces more free volume to accommodate more solvent molecules. This action also induces mechanical stress in the polymer. The mechanical stress can be released by swelling as well as movement and rearrangement of molecular chains.¹

The process described above usually takes some time to accomplish; it is not a fast reaction. When the chemical potential energy and the mechanical stress reach equilibrium state, the mass transfer ends.² The relaxing rate of mechanical stress in a polymer depends on the working temperature. If the working temperature is below the glass-transition temperature (T_g) of the polymer, the polymer is situated at a glassy

state and the relaxing time is prolonged. If the working temperature is above the T_g of the polymer, the polymer is situated at a rubber state and the relaxing time is shortened.³ When a polymer is immersed in an organic solvent, the bonding in its molecular chains weakens. This reduced bonding enhances the molecular chain's mobility and decreases the corresponding T_g .

Hopfenberg and Frish⁴ demonstrated that the diffusive behavior of an organic solvent inside a polymer can be classified into three types: (1) Case I or Fickian diffusion; (2) Case II diffusion; and (3) anomalous diffusion. They are introduced in the following:

1. Case I diffusion: When the diffusive speed of the solvent is much lower than the relaxing rate of molecular chains of the polymer, the absorption balance is achieved immediately. The molecular chains have only local and restrictive movement. There is no swelling in such case.
2. Case II diffusion: When the diffusive speed of the solvent is much higher than the relaxing rate of molecular chains of the polymer, the molecular chains have large-scale movement to produce swelling. More mass transfer occurs after swelling.
3. Anomalous diffusion: When the diffusive speed of the solvent is about the same as the relaxing rate of molecular chains of the polymer, both Case I and Case II diffusions proceed at the same time.

Some researchers^{5–6} reported that the diffusive behavior of polymers in a glassy state belongs to the

Correspondence to: C. B. Lin (cblin@mail.tku.edu.tw).

Contract grant sponsor: National Science Council, Taiwan, Republic of China.

anomalous diffusion. According to Alfrey et al. and Thomas et al.,⁷⁻⁸ the anomalous diffusion can be further divided into three regions: swelling region, unswelling region, and mixed region. At the beginning, the solvent weakens the molecular chains of the polymer to undergo stress relaxation and produce more free space inside the polymer. This free volume allows more solvent molecules to enter until equilibrium is reached. The probability for the solvent molecules to enter or leave the polymer surface is equal. However, if the solvent concentration inside and outside of the polymer is different, the accompanying difference in chemical potential energy forces mass transfer to proceed.

As a polymer changes from a glassy state to a rubber state, its diffusion coefficient increases dramatically. The diffusive process inside a polymer weakens the bonding of molecular chains and produces swelling. Swelling generates a large-scale movement of molecular chains of the polymer and increases its volume. This increased volume generates more free space for the solvent to enter. The polymer therefore translates from a glassy state to a rubber state.^{9,10} For example, Nicolais et al.¹¹ demonstrated that polystyrene's T_g drops from 100 to 20°C, when it is immersed in pure hexane solvent.

This article studies the methanol- and ethanol-induced convex deformation in PMMA experimentally. Both single- and double-convex deformations were produced. The mechanism and factors that influence the deformation process were explored and discussed. A wet phase-inversion method was also used to produce porous convex deformation in poly(methyl methacrylate) (PMMA). The size, number, and location of the convex pores can be prescribed. A variety of asymmetric membrane structures, such as open-cell sponge, closed-cell sponge, and macrovoids, can be fabricated by using the wet phase-inversion method.^{12,13}

EXPERIMENTAL

Absorption study of PMMA

Rectangular samples with $20 \times 10 \times 1$ mm dimensions were cut from PMMA sheets to study the solvent absorption rate of PMMA with inherent viscosity of 0.284 dL/g. These PMMA samples were annealed in the air at 120°C for 24 h and then furnace-cooled to room temperature to release the residual stress. The residual stress came from machining. The solvent absorption of PMMA and PC samples was conducted by measuring the weight gained by the samples at different time intervals. Each sample was preheated to 60°C before being put into the methanol or ethanol. The glass cup which contained the methanol or ethanol was placed in a thermostatic water bath to maintain its

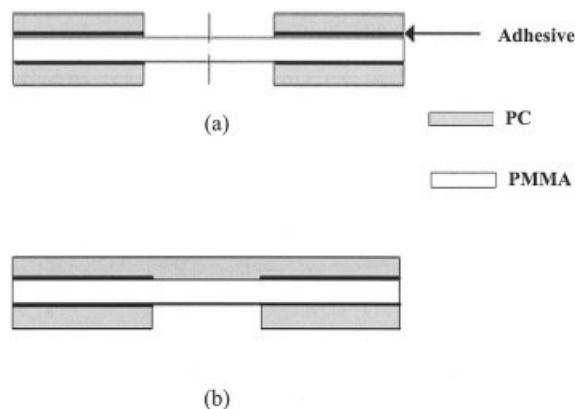


Figure 1 The schematic diagrams of (a) a double-hole and (b) a single-hole sandwich structures.

temperature at 60°C. The sample was removed from the solvent at a fixed time interval, blotted, and then weighed in a ± 0.1 mg digital balance. After weighing, the sample was quickly put back into the solvent to continue the absorption test.

Glass-transition temperature

The experimental procedure for measuring the effective T_g of PMMA in methanol and ethanol is described below. Circular samples having 0.4 mm thickness were punched from PMMA sheets. The samples were annealed at 120°C for 24 h to eliminate the residual stress. The samples were immersed in methanol (or ethanol), which was maintained at 60°C in a thermostatic water bath, until diffusion saturation was reached. Each solvent-saturated sample, having a mass of ~ 10 mg, was then blotted and placed in an aluminum pan. The pan was placed in a Seiko 1 SSC-500 differential scanning calorimeter (DSC) to determine the effective T_g at a scanning rate of 5°C/min.

Mass transport of sandwich structures

Sandwich structures with various hole diameters and PMMA layer thicknesses were tested for comparisons. Figure 1 illustrates the schematic diagram of the sandwich structures [polycarbonate (PC)/PMMA/PC]. Both outer layers were PC and the inner layer was PMMA. The reason for using PC as the outer layers was that PC does not easily interact with methanol or ethanol; thus, it can be regarded as an insulator for the PMMA region where interaction is to be avoided. Two PC layers were glued on the two sides of a PMMA layer by using epoxy adhesive to construct a sandwich structure. Two types of sandwich structures were made. The first type had one hole on both sides of the outer PC layers, as shown in Figure 1(a). The solvent could diffuse into PMMA through these two holes.

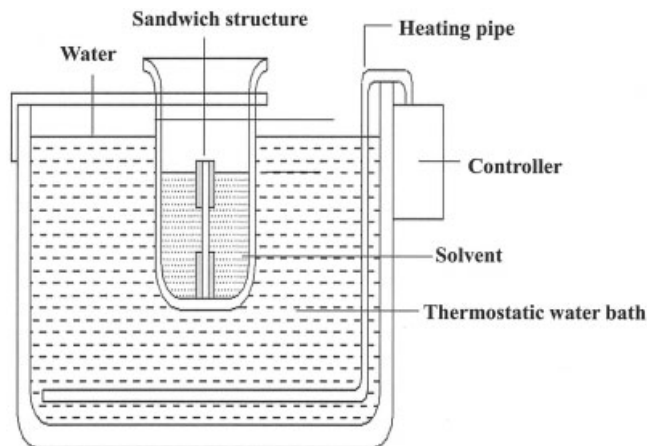


Figure 2 The schematic diagram of the solvent transport in sandwich structure.

The two holes on both sides had the same diameter and were aligned on the same axis. The second type had only one hole on one outer PC layer, as shown in Figure 1(b). The solvent could diffuse into PMMA through only one hole.

Figure 2 illustrates the schematic diagram of solvent transport in sandwich structure. Methanol and ethanol were used as the solvents. PMMA and PC do not dissolve in methanol and ethanol. The relative equilibrium solubility of methanol and ethanol in PMMA at 60°C are 53 and 67%, respectively. However, the corresponding values for PC are only 3 and 7%, respectively. Therefore, these two solvents can diffuse into PMMA much easier than into PC. Each sandwich structure was preheated to 60°C in the thermostatic

water bath before being put into the solvent, which was maintained at 60°C. After the PMMA region exposed to the solvent reached saturation, the sandwich structure was taken out from the solvent. It was then placed on a pan at room temperature until the PMMA layer converted to its glassy state. The two outer layers were removed and the swelling deformation of the PMMA layer was measured by using a Nikon Optiphot-100 optical microscope.

Wet phase-inversion study

The double-hole sandwich structures were also used to study the effect of wet phase inversion. PMMA samples with 1.0 mm thickness and 3.0-mm hole diameter were tested. The sandwich structure was preheated in the thermostatic water bath to 60°C. It was then immersed into the 60°C ethanol until saturation was reached in PMMA. The solvent-saturated sandwich structure was quickly immersed into a 60°C distilled water bath. After precipitation, the sandwich structure was taken from the water bath and dried in the air. The microstructure of the precipitated PMMA was examined by using a LEO-1530 scanning electron microscope (SEM, Seiko Instruments, Inc., Japan).

RESULTS AND DISCUSSION

Figure 3 depicts the result of solvent absorption transport of PMMA. The weight gained by PMMA due to the diffusive transport of methanol or ethanol into PMMA is depicted as a function of absorption time. Notice that in this absorption study only PMMA sam-

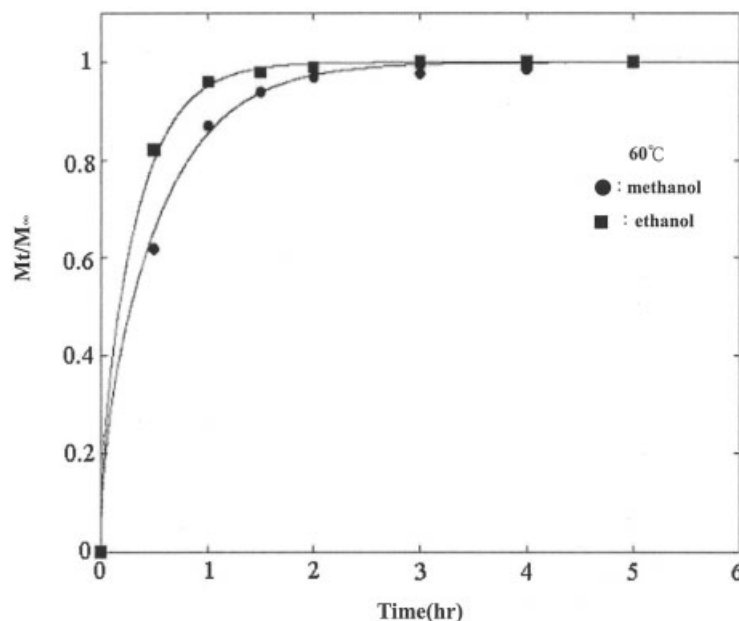


Figure 3 Solvent absorption in PMMA. Solid lines determined by eq. (1). Points are experimental data.

TABLE I
The Effective Glass-Transition Temperature, D , v , and Equilibrium Solubility for the Methanol and Ethanol Transport in PMMA at 60°C

Solvent	$T_{g\text{eff}}$ (°C)	Diffusion coefficient $D \times 10^8$ (cm ² /s)	Diffusion speed $v \times 10^6$ (cm/s)	Equilibrium solubility (%)
Methanol	20.4	30.9	9.8	53
Ethanol	17.6	48.1	3.5	67

ples were used; there were no outer PC layers. Harmon et al.^{14,15} proposed a correlation to predict the anomalous diffusion. The correlation is written below and is also depicted in Figure 3 for comparison,

$$\frac{M_t}{M_\infty} = 1 - 2 \sum_{n=1}^{\infty} \frac{\lambda_n^2 (1 - 2 \cos \lambda_n) \exp\left(\frac{-\nu \lambda}{2D}\right)}{\beta_n^4 \left(1 - \frac{2D}{\nu \lambda} \cos^2 \lambda_n\right)} \exp\left(-\beta_n^2 \frac{Dt}{l^2}\right) \quad (1)$$

In the above equation, M_t is the weight gained due to absorption after a time interval t and M_∞ is the final weight of the sample after the equilibrium state is reached. The parameter D is the diffusion coefficient for Case I diffusion and v is the diffusion speed for Case II diffusion. These two parameters for the materials used in this study are listed in Table I. The parameter l is half the sample thickness. The parameters λ_n and β_n can be obtained from the solutions of the following expressions:

$$\lambda_n = \frac{\nu \lambda}{2D} \tan \lambda_n$$

$$\beta_n^2 = \frac{\nu^2 \lambda^2}{4D^2} + \lambda_n^2$$

As illustrated in Figure 3, the experimental data agree quite well with the prediction, using eq. (1). The coefficients listed in Table I also demonstrate that, for PMMA, Case I diffusion is stronger in ethanol than in methanol, whereas Case II diffusion is stronger in methanol than in ethanol. The equilibrium solubility, the diffusivity at infinite time, in ethanol is also larger than in methanol.

The results of mass transfer in the double-hole sandwich structures are discussed next. Each sandwich structure was first immersed in methanol, which was maintained at 60°C. After saturation, the sandwich structure was removed from methanol and desorbed in the air at room temperature. The PMMA layer returned to its glassy state at room temperature. A double-convex deformation generated when the hole diameter was ≤ 3 mm, as shown in Table II. Figure 4

illustrates the evolving process of the double convex and its physical mechanism is explained next.

The effective T_g 's of PMMA, in methanol and ethanol, are 20.4 and 17.6°C, respectively, as listed in Table I. The effective T_g is less than the solvent temperature, which was maintained at 60°C. The PMMA layer was in its rubber state when immersed in the solvent. The solvent molecules diffused into PMMA, forcing the PMMA molecules to expand and migrate, and induced a mechanical stress. This mechanical stress is called swelling stress in this study. The swelling stress was not symmetrical because the structure of molecular chains in PMMA was not symmetrical. This asymmetrical swelling stress was able to conquer the resistance of the PMMA layer and pushed it towards the topside, as shown in Figure 4(b). The swelling stress reached equilibrium with the reactive stress of the PMMA layer after some time. The topside therefore stopped deforming. The lower side, however, had not reached equilibrium, so that it continued to deform, as illustrated in Figure 4(c). The deformation in the lower side continued until saturation was reached, as shown in Figure 4(d). At saturation, the swelling stress was balanced by the deformation resistant reactive stress of the PMMA layer. The sandwich structure was removed from the solvent after it reached saturation state. It was then dried in the air at room temperature. The two outer PC layers were taken off to measure the convex deformation. Figure 4(e) depicts the schematic diagram of a double convex. Figure 4(f)

TABLE II
The Effect of Hole Diameter on the Formation of Convex Deformations, PMMA thickness = 1.2 mm

	Diameter (mm)				
	3.5	3.4	3.3	3.2	3.1
Cap-structure					
Methanol	Single	Single	Single	Single	Single
Ethanol	Single	Single	Single	Double	Double
	Diameter (mm)				
	3.0	2.9	2.8	2.7	2.6
Cap-structure					
Methanol	Double	Double	Double	Double	Double
Ethanol	Double	Double	Double	Double	Double

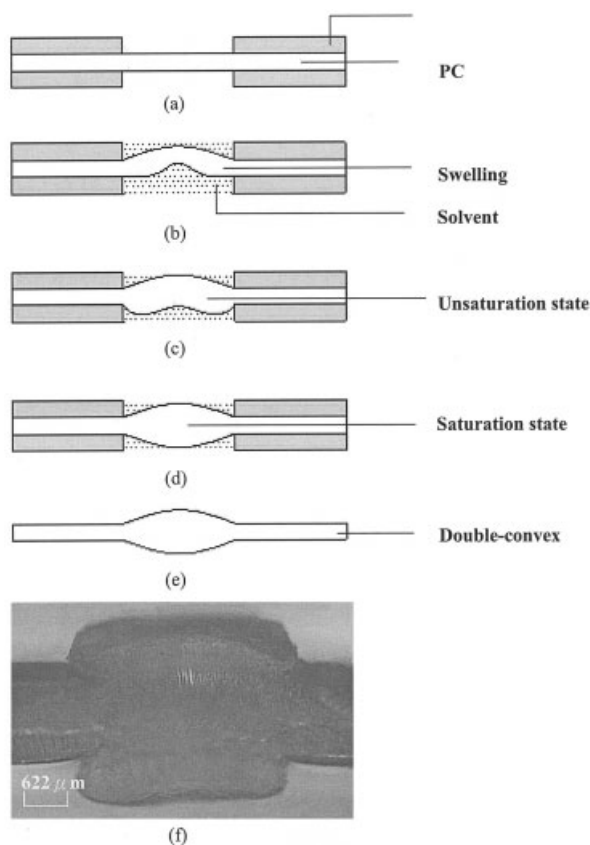


Figure 4 The evolving process of a double-convex deformation.

illustrates the cut-off picture of a double convex. The inside of the double convex is a solid structure. From a mass conservation point of view, the density of the convex is less than the original PMMA. Figure 5 shows a picture of a double convex.

To study the effect of hole diameter on the interaction between PMMA and the solvent, double-hole sandwich structures with various hole diameters were tested. Methanol was first used as the solvent. The results are listed in Table II. When the diameter of the double-hole sandwich structures was larger than 3 mm, a single-convex deformation developed. The physical mechanism of the deforming process of a

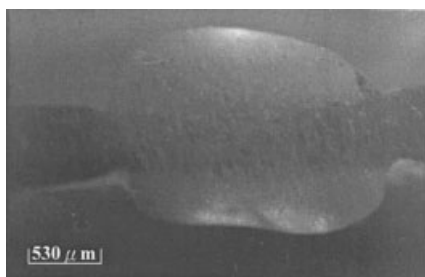


Figure 5 Photograph of a double-convex deformation for a double-hole sandwich structure.

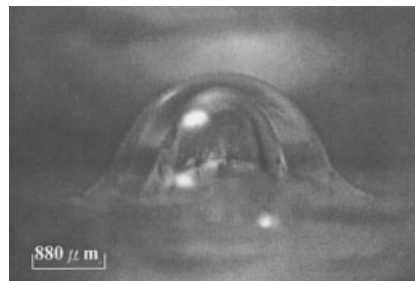


Figure 6 Photograph of a single-convex deformation for a double-hole sandwich structure.

single convex is similar to that described for the double convex. However, the major difference was that the hole diameter became larger. A circular membrane with larger diameter is less capable of resisting deformation. The swelling stress induced by the solvent diffused into PMMA was able to push the membrane further towards the topside, as shown in Figure 4(b). The extent of deformation was too large, and only a single convex developed. The space generated due to the deformation of the PMMA layer towards the topside was large enough to accommodate the space needed for the diffusion in the lower side. There was, therefore, no convex on the bottom side. Figure 6 shows a picture of a single convex. We also conducted the experiment described in the last paragraph with a different solvent, ethanol. All the other parameters were unchanged when the diameter of the double-hole sandwich structures was >3.2 mm, as shown in Table II.

A single-convex deformation with less curvature was developed for the sandwich structure with only one hole on one side, as shown in Figure 1(b). In this case, a PC layer blocked one side of the structure and the PMMA layer was not able to deform as in the double-hole case. The solvent was diffused into PMMA through only one hole and generated a single convex. Without the benefit of deformation, the convex was therefore shorter and less curved. Figure 7 shows a picture of a single convex for a single-hole sandwich structure.

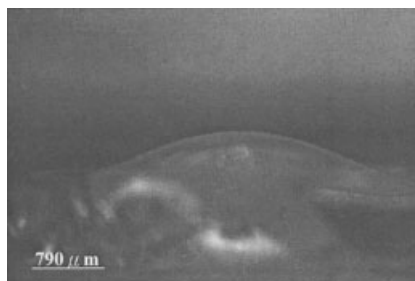


Figure 7 Photograph of a single-convex deformation for a single-hole sandwich structure.

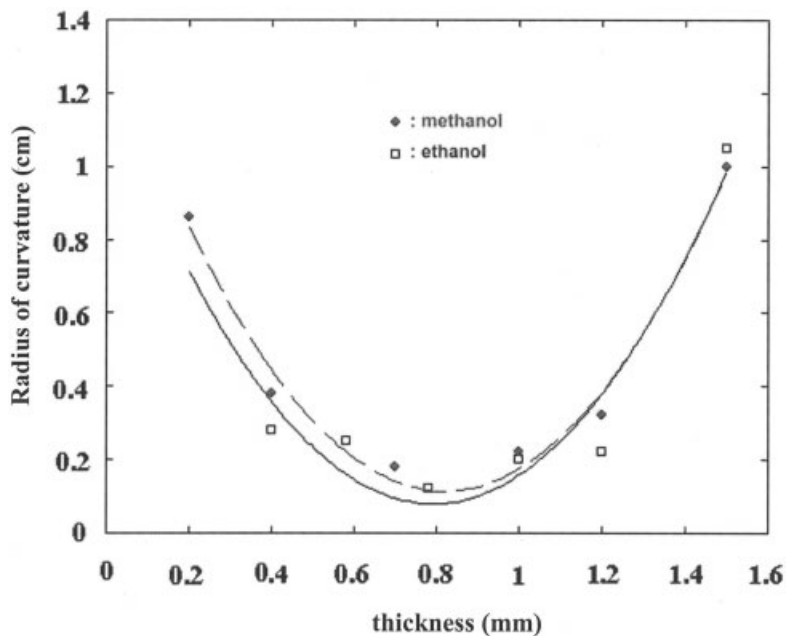


Figure 8 The radius of curvature for the single-convex deformation is depicted as a function of PMMA thickness, hole diameter = 4 mm.

To study the effect of PMMA layer thickness on the interaction of PMMA and the solvent, double-hole sandwich structures with various PMMA thicknesses

were tested. The hole diameter was fixed at 4 mm. The deformations produced were all single convex. The forming time of a convex differed for different PMMA

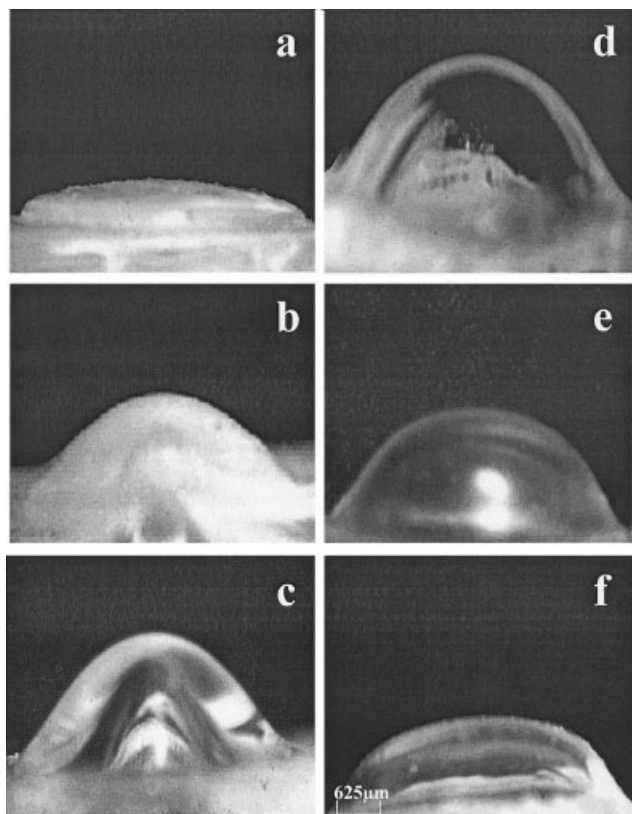


Figure 9 The effect of PMMA layer thickness on convex curvature subject to the methanol, the PMMA layer thickness was (a) 1.5 mm; (b) 1.2 mm; (c) 1.0 mm; (d) 0.7 mm; (e) 0.4 mm; (f) 0.2 mm.

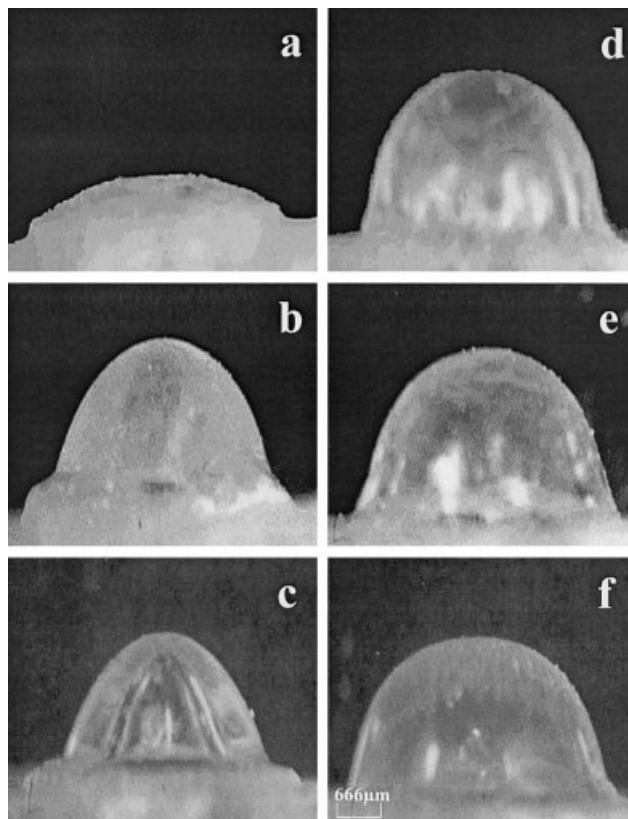


Figure 10 The effect of PMMA layer thickness on convex curvature subject to the ethanol, the PMMA layer thickness was (a) 1.5 mm; (b) 1.2 mm; (c) 1.0 mm; (d) 0.78 mm; (e) 0.6 mm; (f) 0.4 mm.

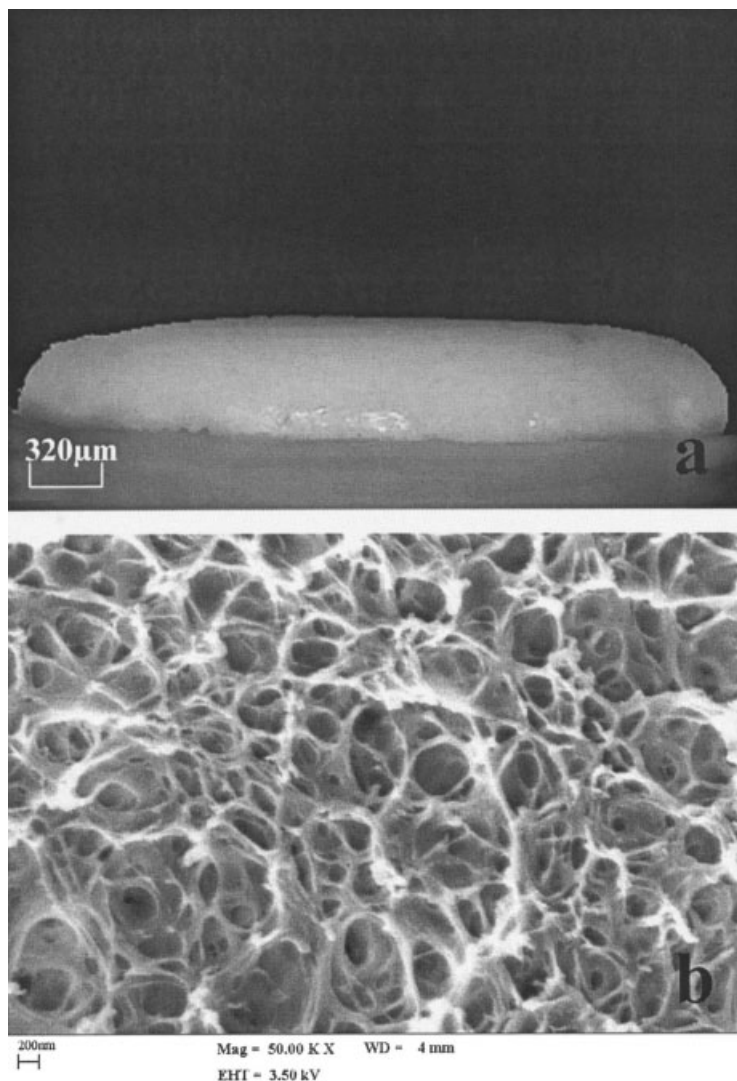


Figure 11 Photographs of (a) a porous single-convex deformation with macrovoid; (b) macrovoid structure inside convex pores. Solvent = ethanol; coagulant = water.

thicknesses. The corresponding forming times in methanol for the thicknesses of 1.2, 1.0, 0.7, 0.4, and 0.2 mm were 12, 10, 7, 4, and 2 h, respectively. The swelling deformation rate of PMMA was about 100 μm/h. Figure 8 depicts the radius of curvature for the single-convex deformation of the double-hole sandwich structures at six different PMMA layer thicknesses. We observe that the maximum curvature and therefore the minimum radius of curvature of the single convex produced in the test occurred when the PMMA thickness was about 0.8 mm for both methanol and ethanol solvents. Increasing or decreasing the PMMA thickness reduced the single-convex curvature. The reasons are explained below.

When the PMMA thickness was larger than about 0.8 mm, there was more content of organic solvent diffuses into the free volume of PMMA. This enhanced mass transfer increased the swelling stress and

the corresponding single-convex curvature. Meanwhile, a thicker PMMA was more capable of resisting deformation. This increased resistance reduced the convex curvature. Figure 9(a–c) illustrates the pictures of the single convexes at three different thicknesses, 1.5, 1.2, and 1.0 mm. The solvent was methanol. Apparently, as demonstrated by the experimental results, the increase in deformation resistance outweighs the increase in swelling stress so that the convex curvature reduces when the thickness increases. Similar results were obtained when ethanol was used as the solvent. Figure 10(a–c) illustrates similar pictures of the single convexes, obtained by using ethanol as the solvent.

When the thickness was less than about 0.8 mm, there was less room for the solvent to enter. This reduced mass transfer decreased the swelling stress and the corresponding convex curvature. At the same time, a thinner PMMA layer was less capable of re-

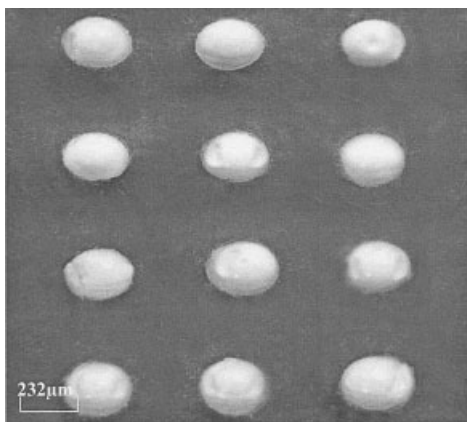


Figure 12 Photograph of double-convex pores matrix produced by using the wet phase-inversion method, each hole diameter was 3.0 mm. Solvent = ethanol; coagulant = water.

sisting deformation and increased the corresponding convex curvature. Figure 9(d–f) illustrates the pictures of the single convexes at three different thicknesses, 0.7, 0.4, and 0.2 mm. The reduction in swelling stress outweighs the reduction in deformation resistance. The convex curvature therefore reduces. Figure 10(d–f) shows similar pictures of the single convexes by using ethanol as the solvent.

The double-hole sandwich structures were also used to study the effect of phase inversion. The test conditions were described in the Experimental. A porous double convex was produced as illustrated in Figure 11. The hole diameter was 3.0 mm. It can be seen that macrovoids were formed in the double convex, because of the ethanol diffused out of the ethanol-saturated PMMA and the coagulant (water) diffused into the PMMA during phase inversion treatment, which results in phase transition and PMMA precipitation to form macrovoids in the double convex. Additionally, the addition of surfactant (coagulant) reduced the interfacial tension between the polymer and the coagulant. The reduction of the interfacial tension induced interfacial instability and initiated the formation of macrovoid, as suggested by Matz.¹⁶ When the ethanol diffused out of the ethanol-saturated PMMA, the surfactant (water) is not used. The macrovoids grow during air-cooling and desorption, while the PMMA temperature remain above the T_g . Air-cooling, however, is so rapid that the T_g is always reached before macrovoids grow to a size equal to the wavelength of the light.¹⁷ Figure 12 shows a picture of a matrix consisting of 12 double-convex pores produced by using the wet phase-inversion method. The PMMA layer thickness was 1.2 mm and the diameter of each double convex was 2 mm. The diameter, number, and location of the convexes can be prescribed. It demonstrates that we can produce porous area selectively on

a polymeric material. This manufacturing process may have potential applications in selective filtering. We are also exploring its applications in the other areas.

CONCLUSION

The interaction mechanism between PC/PMMA/PC sandwich structures and the solvents, methanol and ethanol, was studied. Both single-convex and double-convex deformations were produced. The formation of single- or double-convex deformation depends on the relative strength of the swelling stress induced by the mass transfer and the deformation resistance of the PMMA layer. When methanol was used as the solvent, a single convex was generated for the double-hole sandwich structures as the hole diameter was >3 mm, and a double convex was generated as the hole diameter was ≤ 3 mm. Similar results were obtained when using ethanol as the solvent, but the critical hole diameter was 3.2 mm. For a fixed hole diameter, there was an optimum PMMA layer thickness, ~ 0.8 mm, which produced the maximum curvature. The reasons can be well explained by the relative strength of the swelling stress and the deformation resistance of the PMMA layer. The wet phase-inversion method was used to produce double-convex porous deformations in the PMMA layer. This method allows us to produce the porous area selectively. It may have potential applications in selective filtering and other areas.

The authors gratefully acknowledge the financial support provided by the National Science Council, Taiwan, Republic of China.

References

1. Fujita, H. in *Diffusion in Polymers*; Crank, J.; Pank, G. S., Eds.; Academic Press: London, 1968; Chapter 8.
2. Silberberg, A. *Macromolecules* 1980, 13, 742.
3. Long, F. A.; Kokes, R. J. *J Am Chem Soc* 1953, 75, 2232.
4. Hopfenberg, H. B.; Frish, H. L. *J Polym Sci, Part B: Polym Phys* 1969, 7, 405.
5. Composto, R. J.; Kramer, E. J. *J Mater Sci* 1991, 26, 2815.
6. Sauer, B. B.; Walsh, D. J. *Macromolecules* 1991, 24, 5948.
7. Alfrey, T.; Gurnee, E. F.; Lloyd, W. G. *J Polym Sci* 1966, 12, 249.
8. Thomas, N. L.; Windle, A. H. *Polymer* 1980, 12, 613.
9. Fujita, H. in *Diffusion in Polymers*; Crank, J.; Pank, G. S., Eds.; Academic Press: London, 1968; Chapter 3.
10. Berens, A. R.; Hopfenberg, H. B. *Polymer* 1978, 19, 489.
11. Nicolais, L.; Drioli, E.; Hopfenberg, H. B.; Tidone, D. *Polymer* 1977, 18, 1137.
12. Mulder, M. *Basic Principles of Membrane Technology*; Kluwer Academic Publisher: London, 1991.
13. Koros, W. J.; Fleming, G. K. *J Membr Sci* 1993, 83, 1.
14. Harmon, J. P.; Lee, S.; Li, J. C. M. *J Polym Sci, Part A: Polym Chem* 1987, 25, 3215.
15. Harmon, J. P.; Lee, S.; Li, J. C. M. *Polymer* 1988, 29, 1221.
16. Matz, R. *Desalination* 1972, 10, 1.
17. Lin, C. B.; Liu, K. S.; Lee, S. *J Polym Sci, Part B: Polym Phys* 1999, 29, 1457.